



ELSEVIER

Contents lists available at [SciVerse ScienceDirect](http://www.sciencedirect.com)

Continental Shelf Research

journal homepage: www.elsevier.com/locate/csr

Research papers

Sea surface temperature in False Bay (South Africa): Towards a better understanding of its seasonal and inter-annual variability

François Dufois^{a,*}, Mathieu Rouault^{a,b}^a Department of Oceanography, Mare Institute, University of Cape Town, Rondebosch 7701, South Africa^b Nansen-Tutu Center for Marine Environmental Research, University of Cape Town, South Africa

ARTICLE INFO

Article history:

Received 24 May 2011

Received in revised form

7 February 2012

Accepted 16 April 2012

Keywords:

Sea surface temperature

False Bay

Benguela upwelling

ENSO

South Africa

ABSTRACT

Two sea surface temperature (SST) products, Pathfinder version 5.0 and MODIS/TERRA are evaluated and used to study the seasonal and the inter-annual variability of sea surface temperature (SST) together with local SST and wind data in the vicinity of False Bay (Western Cape, South Africa). At the monthly scale, differences of up to 3 °C are detected between the two products in the bay. In the northern half of the bay, SST is fairly well explained by seasonality. In contrast, the southern half exhibits a higher inter-annual variability in SST. The southern half of the bay and the Western Cape upwelling system (Cape Agulhas to Cape Columbine) share most of their variance. Furthermore, the inter-annual variability of SST in False Bay is correlated with both the Niño 3.4 index and local wind speed anomalies. El Niño (La Niña) events induce an equatorward (poleward) shift in the South Atlantic High pressure system leading to a weakening (strengthening) of upwelling favourable south-easterly. Those changes induce a warm (cold) SST anomaly along the West Coast of Southern Africa.

© 2012 Elsevier Ltd. All rights reserved.

1. Introduction

False Bay is a coastal embayment located on the south-east coast of Cape Town (South Africa) and opened to the south (Fig. 1). Less than 100 m deep, it has an almost rectangular shape with an approximate dimension of 35 × 30 km. The shore of the bay is a huge residential area with a growing population of several million people, and is subject to various environmental issues inclusive of coastal erosion (Brundrit G., Pers. Com.), pollution (Brown et al., 1991; Skibbe, 1991; Taljaard et al., 2000) and associated red tides (Horstman et al., 1991; Pitcher et al., 2008). The description of the physical processes within the bay is thus a prerequisite to help to manage and protect the coastal area.

False Bay lies in a unique location, situated between the warm Agulhas Current and the cold Benguela Current and associated upwelling (Largier et al., 1992). The general concept is that both systems influence the hydrodynamic processes within False Bay. Following Shannon et al. (1985) and Lutjeharms (1991) False Bay lies in the wind-induced upwelling regime of the south-western coast. Cram (1970) and Jury (1985, 1986) suggested that upwelling off Cape Hangklip, the south-eastern extremity of False Bay, induces a persistent area of cold water in the middle of the bay. Water masses in the bay are also exchanged with those further

outside. Shannon and Chapman (1983) considered that inflow from the south-east is probably dominant. Indeed, Shannon and Chapman (1983) suggested that False Bay could be influenced by the Agulhas Bank circulation as most of the drifters placed in the surface water of the western Agulhas Bank were found to drift towards False Bay.

Various observational studies were also conducted, using satellite imagery or current measurements, on the circulation of the bay (Shannon et al., 1983; Jury, 1985, 1986; Botes, 1988; Gründlingh et al., 1989; Gründlingh and Largier, 1991; Nelson et al., 1991; Gründlingh and Potgieter, 1993). It appears that a large variety of currents occurs with a preference for a clockwise circulation within the bay (Shannon et al., 1983; Botes, 1988). In addition, stratification within the bay was investigated. The water column is almost isothermal everywhere in winter, whereas it is strongly stratified during summer with an 8–9 °C difference between the surface and 50 m depth (Atkins, 1970a, 1970b). A rapid intensification of the thermocline is generally observed in late December (Gründlingh et al., 1989).

Despite those studies, mostly carried out from the seventies to the early nineties, various important issues have not been addressed. For instance, the inter-annual variability of hydrodynamical processes of False Bay or even its annual cycle is not well described. In this paper, we focus on sea surface temperature (SST), a key parameter for instances of red-tide blooms in False Bay (Horstman et al., 1991). Atkins (1970a, 1970b) partly described the SST seasonality within False Bay and Jury (1984,

* Corresponding author. Tel.: +27 21 650 5315; fax: +27 21 650 3979.
E-mail address: Francois.Dufois@uct.ac.za (F. Dufois).

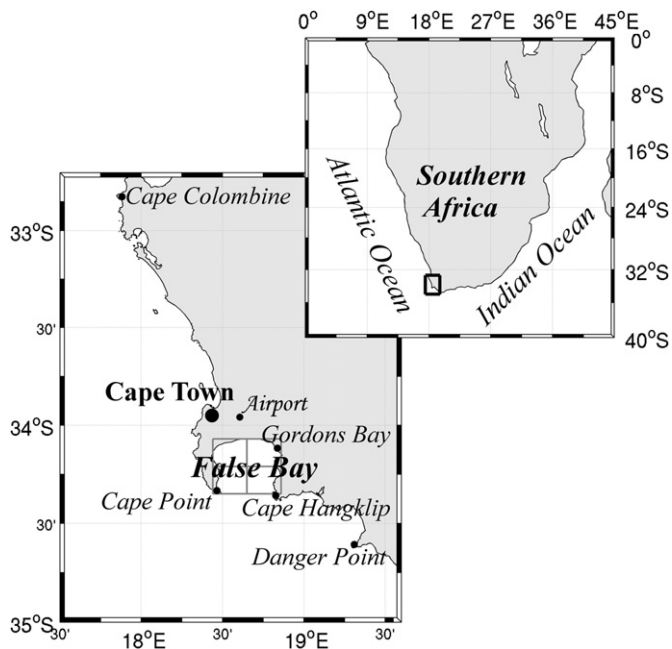


Fig. 1. Study area. The grey boxes over False Bay demarcate the four sectors of the bay discussed within the text.

1985, 1986) described the SST patterns in response to local winds for several case study scenarios. However, almost nothing is known about its inter-annual variability. Only Agenbag (1996) mentioned a potential influence of a 1992 El Niño event on the SST around the Cape Peninsula. At a larger spatial scale, the El Niño Southern Oscillation (ENSO) is known to influence SST in the South Atlantic (Colberg et al., 2004) and around South Africa (Rouault et al., 2010). In this paper, we use satellite remote sensing estimates of SST and *in situ* observations of wind and SST to address the issue. Various SST products are described and evaluated to investigate the annual cycle of SST in the bay. The inter-annual variability is then addressed through Empirical Orthogonal Function (EOF) decomposition and correlation. Afterwards the relationship between SST, ENSO and local wind is investigated. In addition, the relationship between wind, sea level pressure and ENSO both at local and regional scales is discussed.

2. Data

2.1. Data description

SST estimates were obtained from two sources, the Moderate Resolution Imaging Spectroradiometer (MODIS) aboard the NASA Terra satellite and from the Pathfinder 5.0 SST Re-analysis. MODIS sees every point on the earth every one to two days in 36 discrete spectral bands since 2000. Level-2 MODIS data were downloaded from the Ocean Color website (<http://oceancolor.gsfc.nasa.gov>) and processed at a 1 km resolution using the SeaWiFS Data Analysis System (SeaDAS — <http://seadas.gsfc.nasa.gov>). The processing method is described in Dufois et al. (2012). Only the daytime passes were processed, allowing the cloud flag (CLDICE) to be used (SSTWARN and SSTFAIL are not used). The satellite passes over False Bay during the day at around 8:00 UTC, minimizing the impact of solar radiation on skin temperature. Daily data were averaged monthly over the past 11 years. On average, there are about 11 days of good data per month for each grid point over the vicinity of False Bay, with a standard deviation of 3.4 day. The monthly MODIS product used in this study is

validated in the southern Benguela upwelling system off the Cape Peninsula in Dufois et al. (2012).

The Ocean Pathfinder SST project consists in a re-processing of all Advanced Very High Resolution Radiometer (AVHRR) instrument data on board NOAA (National Oceanic and Atmospheric Administration) satellites from 1981 to present with the same algorithm (Kilpatrick et al., 2001). Monthly data were downloaded from the version 5.0 of Pathfinder available at a 4 km resolution (<http://www.nodc.noaa.gov>). In this product, there are eight possible quality levels based on a hierarchical suite of tests, with 0 being the lowest quality and 7 the highest (Kilpatrick et al., 2001). A quality flag of 4, considered as the lowest quality level for acceptable data, was imposed. On average, there are about 5 day of good data per month for each grid point over the vicinity of False Bay with a standard deviation of 2.6 day (daily data were also downloaded for that calculation).

Daily sea surface temperature measured at Gordons Bay (north-east of the bay, cf. Fig. 1) were provided by the South African Weather Service. Those data were available from 1984 to 2007 and were taken in the harbour with a manual thermometer. The monthly SST time series, averaged from the daily data, is used in this study.

Wind speed and direction were provided by the South African Weather Service at Cape Town International Airport and Cape Point (Fig. 1) and used to create monthly wind indices. The upwelling favourable wind in that region is mainly from a south-easterly direction. Thus, the daily wind intensity relative to a north-west/south-east axis, the orientation of the coast, was first calculated and then averaged over one month (hereafter called the monthly south-easterly wind intensity) and was used together with anomaly from a monthly climatological (hereafter called the monthly south-easterly wind anomaly). We also used monthly wind (at 1000 hPa) and pressure (at sea surface) fields at 0.5° resolution from the latest NCEP reanalysis referred to as CFSR (Saha et al., 2010).

2.2. Data evaluation

In order to determine the suitability of each dataset used here, a winter and a summer average of SST was calculated for both products over the common period 2000–2009. SST averages are presented for Pathfinder and MODIS for July/August/September and January/February/March, respectively (Fig. 2(a)). During winter, the two products are similar. During summer, large differences appear, especially on the upwelling cell along the west coast. Pathfinder SST is warmer in the upwelling cell by up to 5 °C and in the northern part of False Bay by up to 3 °C. The climatology done by Demarcq et al. (2003) confirms that the Pathfinder summer climatology (Fig. 2(b)) was too warm. This is in agreement with Dufois et al. (2012) who show that the Pathfinder dataset presents a warm bias during the summer time within the southern Benguela upwelling system. This discrepancy is due to the use of quality flags in Pathfinder SST; quality flags are biased in upwelling regions where large SST gradients are encountered (Dufois et al., 2012). In our region, large SST gradients exist, even more during the upwelling-favorable summer time (Demarcq et al., 2003). Based on that comparison, Pathfinder SST could not be used spatially in the False Bay study area. However, despite the fact that SST gradients are not well reproduced by Pathfinder in False Bay and surrounding water (Fig. 2), it appears that when spatially averaged over the whole False Bay domain, Pathfinder SST matches well with MODIS TERRA SST (Fig. 3(a)). Both monthly values and anomalies from monthly climatology are in good agreement. The correlation coefficients between the two time series are 0.9 and 0.78 and the biases are 0.24 °C and 0.01 °C, respectively. The root mean

square errors are 0.76 °C and 0.5 °C, respectively. Thus, the Pathfinder SST time series averaged over False Bay are considered to be accurate enough which allow us to cover the last 30 years.

MODIS SST is also compared with *in situ* data at Gordons Bay (cf. Fig. 1) situated in the north-east corner of False Bay (Fig. 3(b)). That comparison allows inter-validating both MODIS SST close to

the shore and the *in situ* SST that has been measured manually and daily since 1984. Both monthly SST and anomalies from monthly climatology are in good agreement. The correlation coefficients between the two time series are 0.96 and 0.83, respectively, the bias are 0.25 °C and -0.06 °C, respectively and the root mean square errors are 0.60 °C and 0.49 °C, respectively. Unfortunately, daily SST provided by the South African Weather Service at Fish Hoek, Kalk Bay and Muizenberg in the north-western part of the bay did not lead to such good agreement with MODIS SST (correlations on the anomalies were, respectively 0.60, 0.71 and 0.05) and were dismissed. This might be due to the accuracy of the manual sampling process: data may have been collected in the surf zone or in pools and are not representative of the nearshore SST. However, our results provide ample motivation for the South African Weather Service to continue archiving SST at Gordons Bay in a similar fashion and to upgrade measurement procedures in other locations of False Bay.

3. Results

3.1. Climatology of the sea surface temperature

A monthly climatology of SST in the domain extending from 33.5° to 35°S and from 18° to 19.5°E was generated averaging monthly MODIS SST for the period 2000–2010 (Fig. 4). The south part of the domain is generally warmer. The coastal area of the west coast is generally colder than surrounding water even in winter. Except for one part of the upwelling cell lying west of the Cape Peninsula, SST is generally colder during the winter time. The cold upwelling tongue lying between Cape Columbine and Cape Point is

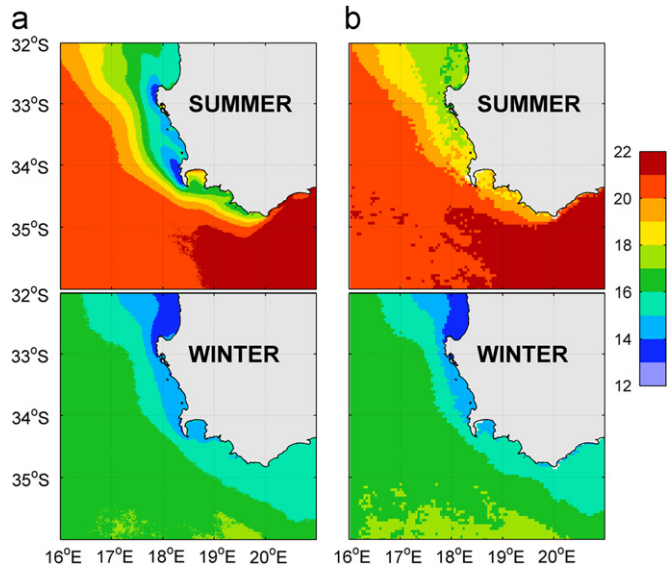


Fig. 2. Average of SST (°C) from 2000 to 2009 during austral summer (top) and winter (bottom) time using MODIS (a) and Pathfinder (b).

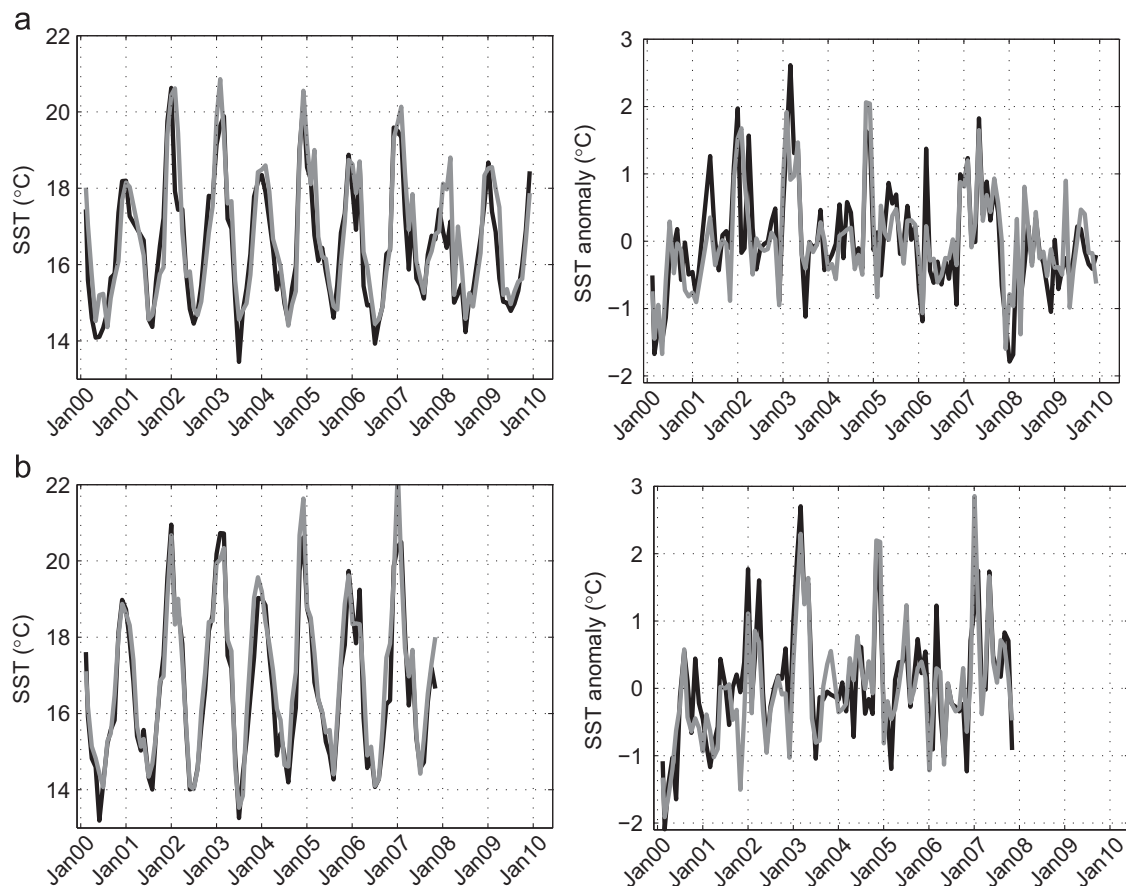


Fig. 3. (a) Comparison of monthly SST (left) and monthly SST anomaly (right) from MODIS (black) and Pathfinder (grey) averaged over the all False Bay domain. (b) Comparison of the SST (left) and the SST anomaly from the climatology (right) from MODIS (black) and *in situ* (grey) SST at Gordons Bay.

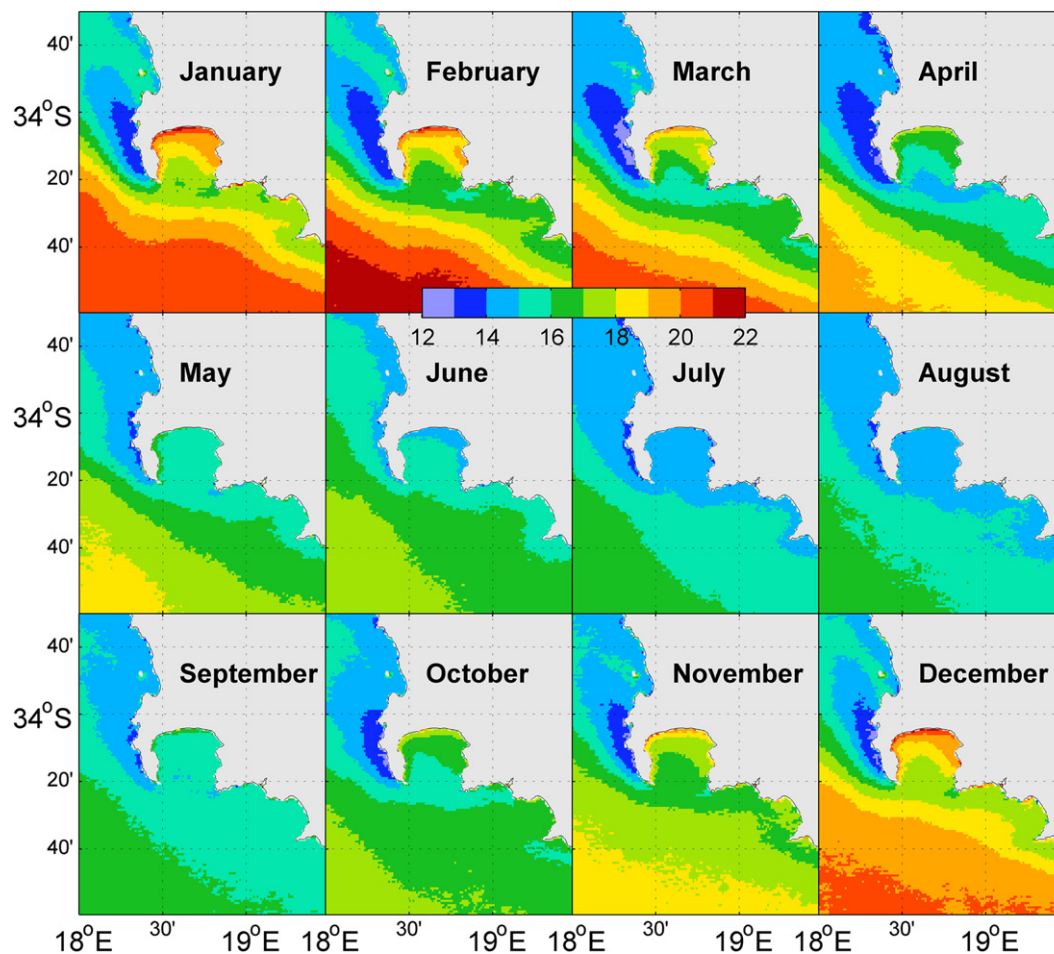


Fig. 4. Monthly SST ($^{\circ}\text{C}$) climatology from 2000 to 2010. Computed with MODIS TERRA data from averaging monthly composites.

Table 1
Mean, maximum (max.), minimum (min.) and standard deviation (SD) of monthly SST considering the whole time series, the summer time (January to March) and the winter time (July to September). MODIS data were averaged over four boxes delimiting the north-eastern, north-western, south-western and south-eastern area of False Bay (the domain $34.07^{\circ}\text{--}34.35^{\circ}\text{S}$ and $18.44^{\circ}\text{--}18.86^{\circ}\text{E}$ was equally divided in four areas). For Gordons Bay the *in situ* time series was used.

	Whole time series				Summer time				Winter time			
	Mean	Max.	Min.	SD	Mean	Max.	Min.	SD	Mean	Max.	Min.	SD
NE False Bay	16.8	21.0	13.4	2.0	18.8	21.0	15.5	1.3	14.8	16.3	13.4	0.7
NW False Bay	16.9	21.4	13.6	1.9	18.8	21.4	16.4	1.2	15.0	16.6	13.6	0.7
SW False Bay	16.1	20.2	13.5	1.4	17.2	20.2	14.9	1.3	14.9	16.2	13.5	0.6
SE False Bay	16.2	20.6	13.3	1.6	17.6	20.6	14.7	1.3	14.8	16.0	13.3	0.6
Gordons Bay	16.6	22.5	12.7	2.0	18.4	22.5	15.4	1.4	14.6	16.5	12.7	0.9

visible from October to April and exhibits SST around $13\text{--}14^{\circ}\text{C}$ at the monthly scale during summer. The rest of the domain shows a “normal” seasonality with warmer SST during summer. Within the domain the strongest amplitude is observed in the northern half of False Bay, whose SST varies from about 14 to $21\text{--}22^{\circ}\text{C}$. The southern half of False Bay displays less amplitude with SST varying from about 14 to $19\text{--}20^{\circ}\text{C}$. A strong gradient of SST occurs from October to April across False Bay. A cold water tongue separates coastal water from offshore water in surface during summer. From May to September the SSTs are more homogeneous within the bay.

In order to give some SST characteristics over the past years, False Bay was divided in four equal areas (Fig. 1) and four spatially averaged SST time series were extracted. Table 1 shows several statistical parameters for each area which confirm the previous findings. The northern half of the bay exhibits SST

ranging from 13.4°C to 21.4°C at a monthly scale over the past 11 years whereas the southern half of the bay has values ranging from 13.3°C to 20.6°C . The northern bay displays higher amplitude variation and a higher standard deviation. It also appears that the variability, represented by the standard deviation, is globally higher during summer. Winter displays lower variability, and also more homogeneity throughout the four sectors of the bay. Gordons Bay time series properties are coherent with those of the north-western sector of False Bay. There, SST has high amplitude with values ranging from 12.7°C to 22.5°C .

3.2. Inter-annual variability of the SST

In order to quantify the significance of the climatology and investigate inter-annual variability in the region, variance of

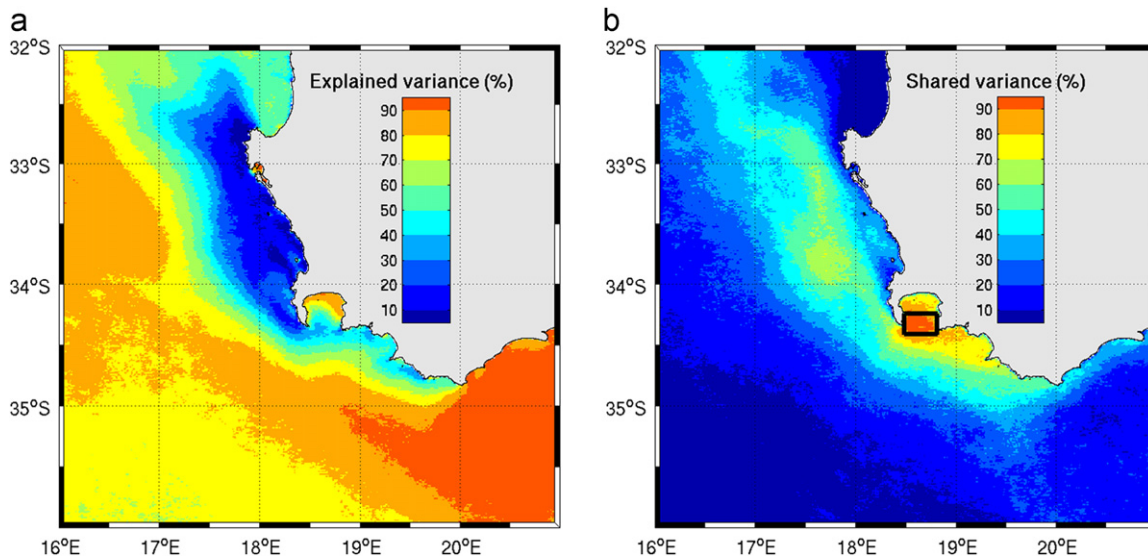


Fig. 5. (a) Variance (%) of monthly SST explained by the monthly climatology. (b) Variance (%) of the monthly SST anomaly in the entire domain shared with monthly SST anomalies averaged over the black box.

monthly MODIS SST explained by monthly climatology was computed (Fig. 5(a)). For each grid point, this value corresponds to the square of the correlation coefficient between the monthly SST time series and the monthly climatological time series. Most of the monthly variance ($> 70\%$) is explained by the annual cycle on the northern half of the bay. On a larger scale, it appears that offshore SST in our domain study is also fairly well driven by seasonality. On the contrary, neither the upwelling cell along the west coast of the peninsula nor the southern part of False Bay appears to be driven by seasonality. This can be expected from an upwelling region.

In order to investigate the origin of the inter-annual variability in False Bay, a time series of SST anomaly from monthly climatology averaged over the southern half of False Bay (*cf.* Black box in Fig. 5(b)) was extracted. The variance shared in our domain study with that time series is presented on Fig. 5(b). Fig. 5(b) displays the square correlation coefficient between monthly SST anomaly for each grid point and the time series of monthly SST anomaly averaged over the black box. Thus, the inter-annual variability in southern False Bay appears to be shared with the upwelling along the west coast from Cape Agulhas to Cape Columbine. Moreover there were apparently no links between SST variability in False Bay and the open ocean, suggesting that variability in False Bay is mostly due to local processes or driven by the upwelling system surrounding False Bay.

3.2.1. Empirical orthogonal function (EOF) analysis

An EOF (Legendre and Legendre, 1998) was performed on the monthly SST anomaly field of the region extending from 33.5° to 35° S and from 18° to 19.5° E (Fig. 6). The spatial pattern of the two first modes was retained, which collectively explained about 73% of the variance. Their corresponding time coefficients are presented (Fig. 6). The first mode, representing about 64% of the variance, is largely predominant. The spatial structure of that mode (Fig. 6(a)) is quite homogeneous over the region. On the contrary the spatial pattern of the second mode (Fig. 6(b)), explaining about 9% of the variance, exhibits a dipole which distinguishes two areas, the coastal zone including the west coast upwelling and False Bay and a more offshore zone.

The principal component (PC) time series associated with those two modes shows a strong month-to-month variability

(Fig. 6(c)). No significant correlations were found between those PC time series and any other time series representing large scale and local forcing, for instance El Niño Southern Oscillation (ENSO), Antarctic Annular Oscillation, Atlantic Meridional Overturning, and south-easterly wind indices. However, only 11 years of data were available which means that each monthly correlation was done with only 11 points. In addition, there were only on average 11 good days of data per month. In order to bypass that technical problem, we applied a 3-monthly running mean to the time series in order to remove the highest frequency and have more consistent values to perform the correlation (Fig. 7(a) and (c)). Indeed, the filtered first PC (PC1) is correlated with the Niño 3.4 index with a coefficient of 0.59, and the filtered PC2 is correlated with the filtered south-easterly wind anomaly at the Cape Town airport with a coefficient of 0.67 (a lower coefficient of 0.43 is found using wind anomaly at Cape Point). Best correlations with the Niño 3.4 index are found by imposing a four month lag to the time series. Looking at the monthly dependency of those correlations, the correlations between ENSO and the PC1 varies from 0.7 to 0.85 from January to May (Fig. 7(b)) in agreement with Rouault et al. (2010). During the rest of the year no significant correlations (p -value > 0.05) are found but early summer correlations varies from 0.4 to 0.6. Significant correlations up to 0.92 are found throughout the year between PC2 time series and our south-easterly wind index at the airport, except from June to August, when the south-easterly is less frequent. This suggests that coastal wind anomalies unrelated to ENSO modulate the SSTs.

3.2.2. Seasonal SST anomalies

3.2.2.1. Relation with the wind. The correlation between south-easterly wind anomaly and SST anomaly from climatology is shown in Fig. 8. Each seasonal correlation was done with a time series composed of 30 to 33 values (for each month there are either 10 or 11 available years and each season is composed of three months). At each grid point, correlations are calculated using wind time series at both Cape Point and the airport, and the best correlation is retained. Highest correlations are found along the west coast in summer (January to March), when south-easterly winds are the strongest and most frequent. The

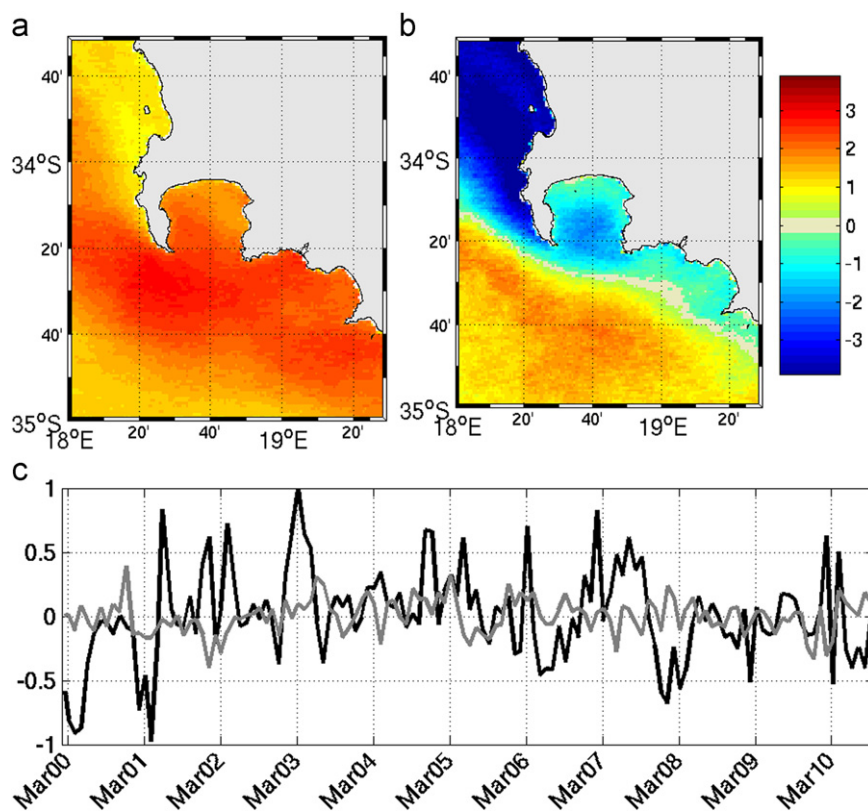


Fig. 6. EOF analysis of MODIS monthly SST anomalies from monthly climatology. (a) First EOF, (b) second EOF and (c) principal component time series of those two EOFs. EOF 1 (black) explains 64% of the variance and EOF 2 (grey) explains 8.8% of the variance.

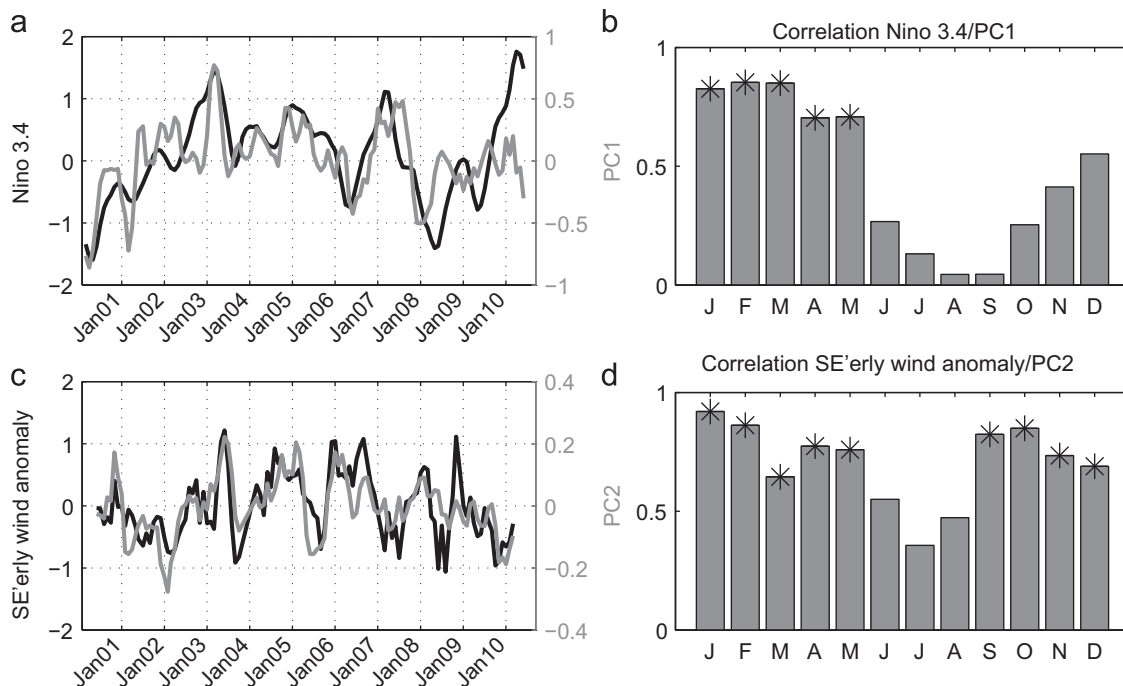


Fig. 7. Comparison between PC1 and Niño 3.4 index (a) and monthly dependency of their correlation (b). Comparison between PC2 and south-easterly wind anomaly (c) and monthly dependency of their correlation (d). A 3-monthly running mean was applied to all time series. The star denotes a statistically significant correlation (p -value ≤ 0.05).

upwelling cells along that coast exhibit significant negative correlations with wind anomaly every season. The correlations are however lower during autumn (April to June). South-west of

False Bay, significant correlations with wind anomaly are only found during summer. In False Bay, SST and wind anomalies are well correlated during summer, notably on the middle of the bay.

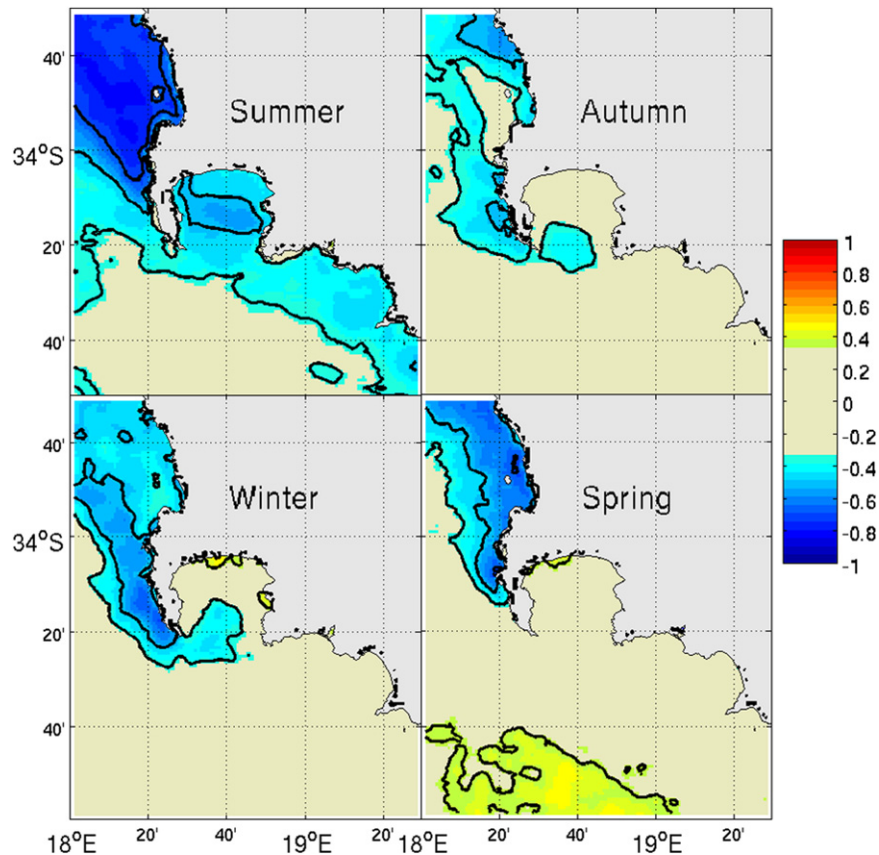


Fig. 8. Seasonal correlations between SST anomalies and south-easterly wind anomaly (at both Cape Point and the airport) for summer (January to March), autumn (April to June), winter (July to September) and spring (October to December). Isocontours 0.35, 0.5 and 0.7 are added. Non-significant correlations (p -value > 0.05) are displayed in grey.

During the rest of the year, significant correlations are only found at the mouth of the bay during winter (July to September) and autumn (April to June). Positive significant correlations are also found alongshore in False Bay in winter and spring (October to December). In general, over the entire region, SSTs exhibit a better correlation with the wind at the airport, while the wind at Cape Point improves the correlation around the Cape Peninsula and the southern section of False Bay (not shown).

3.2.2.2. Relation with ENSO. Seasonal correlation between the Niño.3.4 Index and SST anomaly from climatology is shown in Fig. 9. The four month lag previously applied to the Niño 3.4 index was kept. Significant correlation between the Niño 3.4 index and SST anomalies are observed during summer and autumn and to some extent in spring with higher values in False Bay and in the south of our study domain. Correlations along the west coast north of Cape Point are lower but still significant. No significant correlations are found during winter in the region, whereas the impact of ENSO started during spring south of False Bay.

In order to better ascertain the impact of ENSO over SST in the vicinity of False Bay, composites (average of several seasons) of SST in summer during El Niño years (austral summer 2002/2003, 2004/2005, 2006/2007 and 2009/2010) and La Niña years (austral summer 1999/2000, 2000/2001, 2005/2006, 2007/2008 and 2008/2009) were calculated. The anomaly of SST during those events is presented together with the mean summer SST in Fig. 10. In agreement with results obtained from the EOF decomposition, the impact of El Niño and La Niña on the SST was quite homogeneous over the whole domain. During La Niña years, SSTs are colder everywhere and the upwelling cell is extended, whereas during El

Niño years, SSTs are warmer everywhere and the upwelling cell is reduced but not totally suppressed. Moreover, over the 11-year period, both the cold and the warm absolute anomaly reach up to 1 °C at the seasonal scale. During both events the maximum anomalies are directly south of False Bay. High anomalies, whether warm or cold, are also encountered off the west coast in the upwelling cells, whereas directly along the west coast the anomalies are weaker. Regionally, patches of highest SST anomalies induced by El Niño/La Niña events match areas of strongest SST gradient (Fig. 10(b)).

3.2.2.3. Relation between the SST anomalies and ENSO in False Bay. On average, there is a correlation of 0.43 between Niño 3.4 and monthly SST anomaly over the period 2000–2010 in False Bay, using MODIS data. Applying a 3-monthly running mean to the SST (Fig. 11(a), grey line) increased the correlation to 0.57. The month-by-month correlation using non-filtered data shows (Fig. 11(b)) that correlations are greater during summer. Significant correlations up to about 0.9 occur in February and April, but not in the other summer and autumn months, although correlations are all weakly positive. During the nine El Niños and La Niñas events that occurred during this period, the SST anomaly response was coherent, with a cold anomaly in False Bay during La Niña events and warm anomalies during El Niño (Fig. 11(a)). However, the relationship was not strictly linear; for instance the strong 2009/2010 El Niño events did not induce a high warm anomaly during the austral summer months. Some other anomalies are not linked to ENSO, for example around January 2002, revealing that other processes are also partly responsible for the inter-annual variability. A nonlinear relationship between

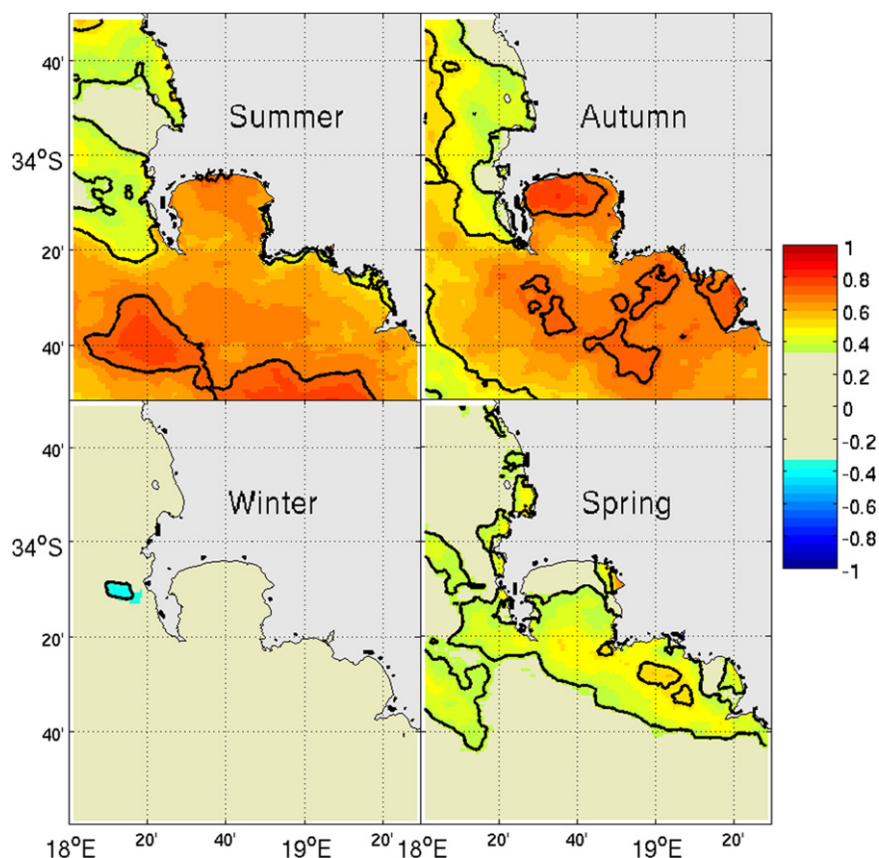


Fig. 9. Seasonal correlations between SST anomalies and the Niño 3.4 index for summer (January to March), autumn (April to June), winter (July to September) and spring (October to December). Isocontours 0.35, 0.5 and 0.7 are added. Non-significant correlations (p -value > 0.05) are displayed in grey.

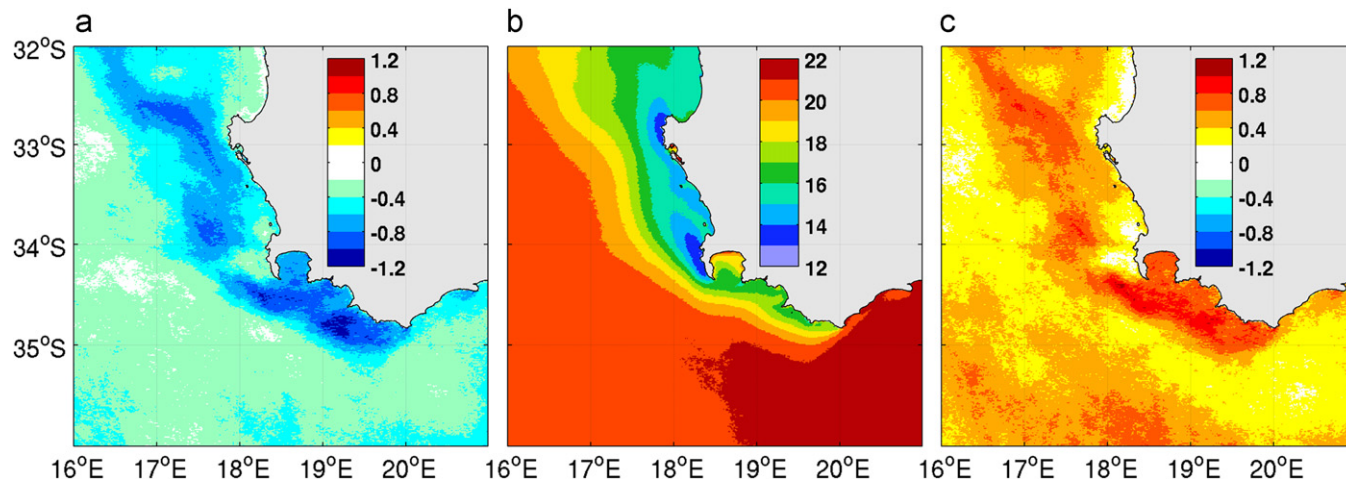


Fig. 10. On average over the summer time (January, February, March): (a) Anomaly of monthly SST ($^{\circ}\text{C}$) during the La Niña years (austral summer 1999/2000, 2000/2001, 2005/2006, 2007/2008 and 2008/2009); (b) Mean monthly SST ($^{\circ}\text{C}$) from 2000 to 2010; (c) Anomaly of monthly SST ($^{\circ}\text{C}$) during the El Niño years (austral summer 2002/2003, 2004/2005, 2006/2007 and 2009/2010).

ENSO and South African or Southern African summer rainfall is also outlined in Rouault and Richard (2003, 2005) and Phillippon et al. (2011). As in the previous section, a four month lag was applied to the Niño 3.4 index. It was found to give the best correlation to the SST time series. Nevertheless, it appeared that for some ENSO events, the 4 month lag was not appropriate. During 2008 a zero-lag would have allowed a better match between the two time series (cf. Fig. 11(a)). In order to extend the previous findings to a longer time scale, Pathfinder and *in situ* SST at Gordons Bay were used. The month-by-month correlations

between the two SST anomaly time series and the Niño 3.4 index are presented in Fig. 11. This analysis confirms the existence of a significant positive correlation between monthly SST anomaly in False Bay and ENSO mainly from January to May. However, considering the whole time series at all months of the year, the correlation is weaker (resp. 0.20 and 0.22 for Pathfinder and the *in situ* data). Considering the time series from 2000 in order to match the MODIS time series, increases the correlation (resp. 0.44 and 0.51). Significant correlations up to 0.5–0.6 are still found during the summer time using the 29 years of Pathfinder data or

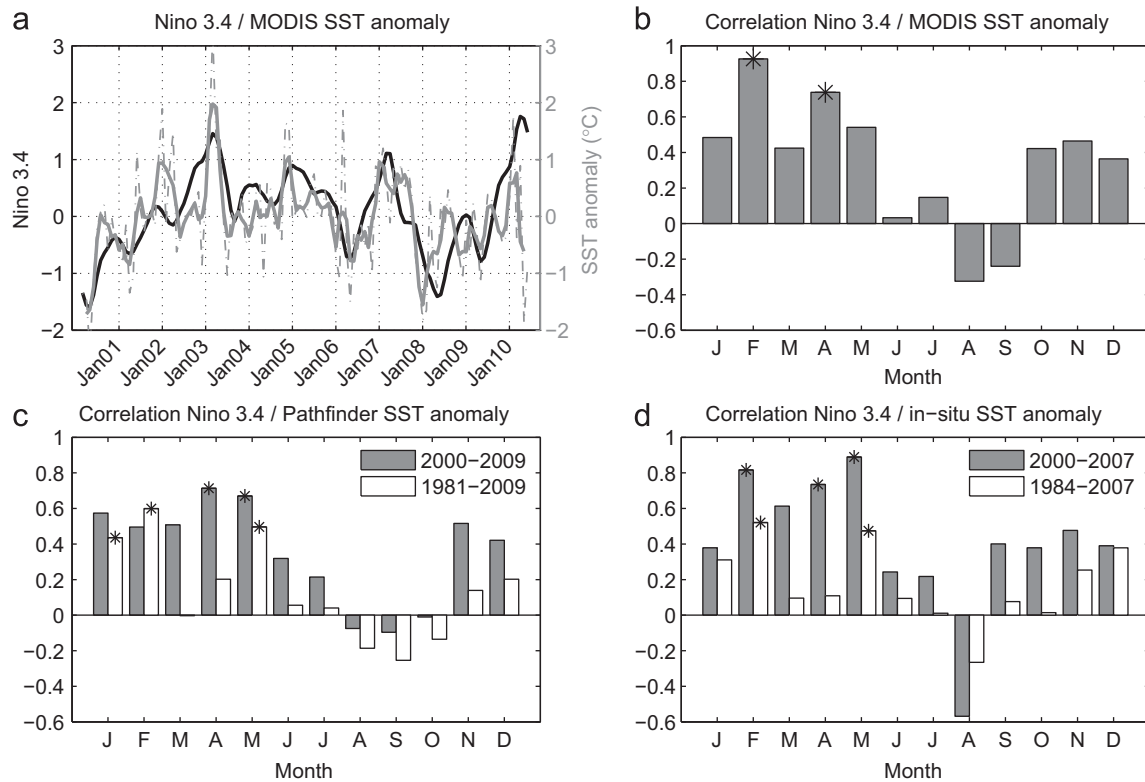


Fig. 11. (a) Comparison between the Niño 3.4 index (black) and monthly SST anomaly ($^{\circ}\text{C}$) derived from MODIS and averaged over False Bay (dashed grey line). The filtered (3-monthly running mean) SST anomaly is added (grey line). (b) Associated monthly dependency of the correlation. (c) Monthly dependency of the correlation between the Niño 3.4 index and monthly SST anomaly derived from Pathfinder and averaged over False Bay from 2000 (grey bars) and from 1981 (white bars). (d) Monthly dependency of the correlation between the Niño 3.4 index and the *in situ* monthly SST anomaly at Gordons Bay from 2000 (grey bars) and from 1984 (white bars). The star denotes a statistically significant correlation ($p\text{-value} \leq 0.05$).

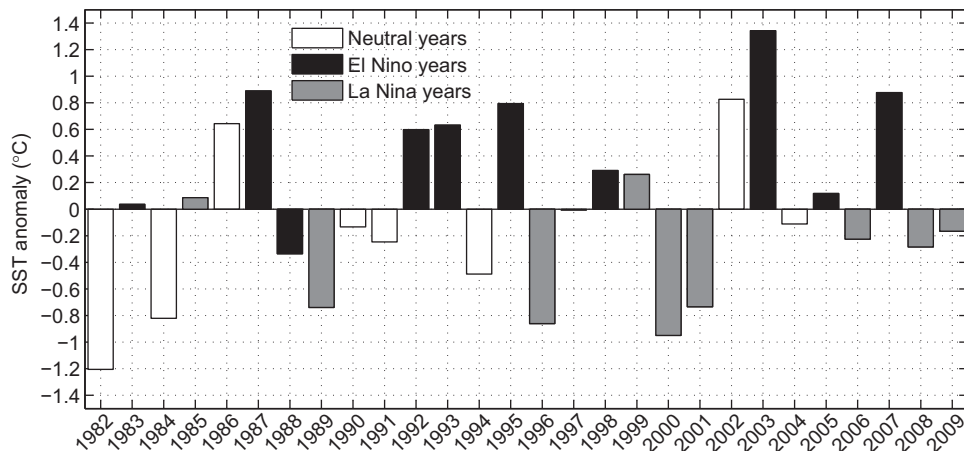


Fig. 12. SST anomaly ($^{\circ}\text{C}$) from the climatology averaged from January to May using Pathfinder over False Bay.

the 24 years of *in situ* data (Fig. 11(c) and (d)). A similar result was found by Rouault et al. (2010) using coarser resolution OISST for a larger domain.

In order to assess more explicitly the relation between cold and warm events in False Bay and La Niña and El Niño years, its non-linearity and potential caveats, the Pathfinder SST anomaly over False Bay was averaged from January to May, months that show the greatest correlation with ENSO. Fig. 12 shows that most of the strong warm anomalies ($> 0.5^{\circ}\text{C}$) happened during El Niño years, except for austral summer 1985/1986 and 2001/2002. Most of the strong cold anomalies ($< -0.5^{\circ}\text{C}$) happened during La Niña years, except for summer 1981/1982 and 1983/1984. However, all the El Niño and La Niña events did not necessarily

induce positive or negative anomalies as during El Niño 1987/1988. Moreover, the amplitude of the SST anomaly within False Bay was not necessarily related to the strength of the El Niño or La Niña events. The strong 1982/1983 or 1997/1998 El Niño events did not induce high warm SST anomaly for instance. Finally, the relationship between ENSO and the SST in False Bay did not appear to be linear, which explains why the correlations are not higher. This result was also found for summer rainfall in South and Southern Africa, regions whose rainfall is usually negatively correlated with ENSO. For instance the 1997/1998 El Niño events did not lead to a major droughts as it was the case for 1982/1983 (Rouault and Richard, 2003, 2005). However, warm (cold) events in False Bay usually happened during El Niño (La Niña).

3.2.3. Relation between wind/pressure anomalies and ENSO

Looking over the 29-year Pathfinder period (1981–2009), we find no significant correlations between the wind at Cape Town airport (in terms of frequency, amplitude, etc.) and ENSO. However, significant negative correlations are found at Cape Point between the Niño 3.4 index and the south-easterly wind anomaly from November to February (Fig. 13). Moreover, during winter, significant positive correlations are found in September. Looking at either the *in situ* data or the CFSR reanalysis gave the same results. This gives confidence in using the CFSR product in our study area. The correlation between ENSO and the south-easterly wind anomaly within the CFSR product is variable at the regional scale. Indeed, during summer, correlations weaken toward the north of Cape Point, and strengthen toward the west (correlation coefficient of about -0.6 were reached at 14°E and 34.5°S). For this analysis no lag is imposed to the Niño 3.4 index, but any lag from 0 to 4 months give about the same results. To assess the mechanisms responsible for change of wind with ENSO, and to further discuss the link with ENSO, the wind and the SST anomalies, a composite of sea level pressure and wind anomaly

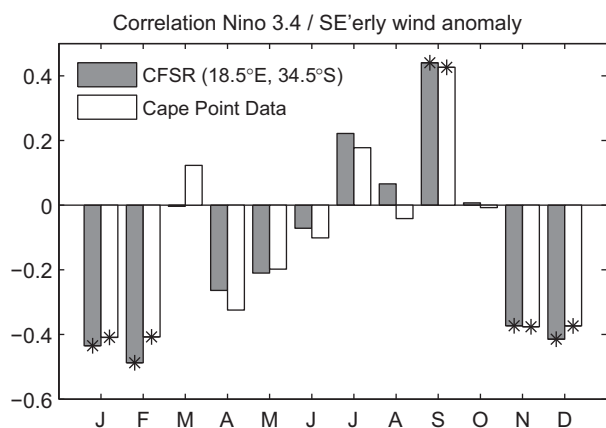


Fig. 13. Monthly dependency of the correlation between the Niño 3.4 index and south-easterly wind anomaly at Cape Point from 1981 to 2009. Grey bars corresponds to the CFSR wind at position 18.5°E and 34.5°S , and white bars to the data from the Weather Service.

during La Niña years and El Niño years is presented on Fig. 14 for summer time (December, January and February). First, we notice a shift in the South Atlantic High pressure system. While the high pressure system shifts poleward in summer during La Niña, it shifts equatorward during El Niño. Over the continent, the low pressure system shifts accordingly. This results in heterogeneous wind anomaly field at the regional scale. As an example, while during La Niña there is a westward increase of the flow at the monthly scale (which coincides to either stronger westward wind or less frequent eastward wind) south of Cape Point, there is a southward increase of the wind along the coast north of 32°S . Around Cape Town and False Bay, La Niña (El Niño) is likely to induce an increase (decrease) of south-easterly wind (at the monthly scale).

4. Discussion and conclusions

Several monthly sea surface temperature (SST) products are used to assess the annual cycle and inter-annual variability in the vicinity of False Bay. The spatial analyses are based on 11 years of MODIS/TERRA SST data owing to its high spatial resolution and its ability to reproduce strong SST gradient in coastal areas. The Pathfinder and the *in situ* SST time series are used conjointly to confirm the findings over a longer time scale (29 and 24 years respectively), particularly the correlations with ENSO. Within False Bay, a bias of up to 3°C in the Pathfinder dataset at the monthly scale during the upwelling season was observed and prevented its spatial use in our study area.

A climatology of False Bay SST is presented for the first time. The shelf waters slightly further offshore south of False Bay are slightly warmer, which could be due to the leakage of Agulhas Current and Agulhas Bank water to the Atlantic Ocean (Lutjeharms and Cooper, 1996). From May to September SSTs are homogeneous within the bay. Around summer-time (October to April), there is coastal upwelling centred on Cape Hangklip, Danger Point and just west of Cape Agulhas (Fig. 10(b)) which separates False Bay from the warm offshore waters. The shallower waters of the northern part of False Bay, where the SST standard deviation is higher, apparently respond to seasonal signals, likely to be sun-warming. The cold water in the south of False Bay seems to originate from the

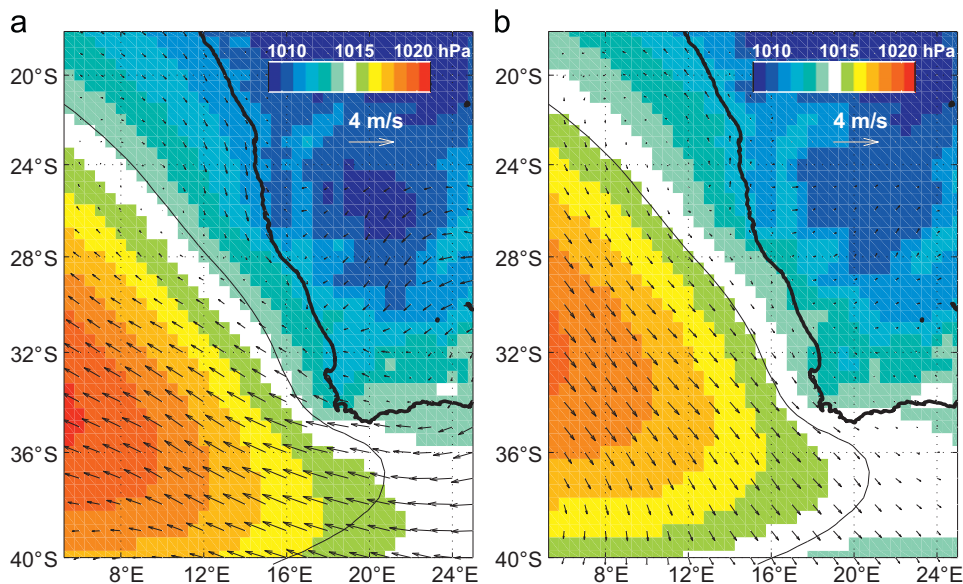


Fig. 14. December to February 1981–2009 average CFSR sea level pressure (hPa) and wind speed and direction composite anomaly (m/s) during La Niña years (a) and during El Niño years (b). The black line shows the climatological 1015 hPa isobar during December/January/February.

upwelling region near Cape Hangklip, as suggested by Cram (1970) and Jury (1985, 1986). The Cape Hangklip upwelling is linked to the upwelling centres west of the Cape Peninsula and off Cape Columbine, all driven by the prevalent south-easterly winds during spring, summer and autumn.

Therefore, the southern half of the bay and the upwelling system (from Cape Agulhas to Cape Columbine) exhibits the same variability. Their seasonality is low and they share most of their variance. The origin of monthly SST anomalies in the vicinity of False Bay is assessed using Empirical Orthogonal Function analysis and correlations. There is a strong impact of ENSO on the SST inter-annual variability even at a local scale such as Gordons Bay. The relation between ENSO and its impact on SST anomalies is not linear, nevertheless most of the coldest (warmest) anomalies happen during La Niña events (El Niño). However, some events did not lead to the expected response. Additionally it appears that the correlation between ENSO and SST anomaly in False Bay has been higher during the last ten years than during the past 30 years. This could happen by chance or it could be related to the increasing intensity and frequency of central Pacific El Niño (Lee and McPhaden, 2010), the region of the Pacific most correlated with South African climate (Fauchereau et al., 2009).

The local wind anomaly at Cape Town airport and Cape Point is also correlated with SST anomaly during the windy summer season. According to Jury (1984, 1985, 1986) strong local effects due to the shape of the coast and the mountains are likely to impact the synoptic wind. The orography surrounding of False Bay then induces important differences between the wind at Cape Point and at the airport (directions can even be opposite). Previous studies stated that the Cape Point data showed more similarities than the airport data with conditions further out to sea at the daily scale (Atkins, 1970a; Andrews and Hutchings, 1980; Jury, 1984, 1985). We however suggest that, when looking at SST inter-annual variability, the anomaly of upwelling favourable wind measured at the airport is a valuable wind index. Indeed, at the scale of the study area (Fig. 8), the south-easterly wind anomaly at the airport is more representative than the one at Cape Point (both correlations with the PC2 and with SST anomalies over the region are higher).

Questions remain on what processes link ENSO and SST variability in the region. There is no link between SST variability in False Bay and the open ocean. ENSO-driven SST variability is rather due to local forcing process or driven by the west coast upwelling. Confirming other studies at a larger scale (Colberg et al., 2004; Rouault et al., 2010), El Niño (La Niña) events induce an equatorward (poleward) shift in the South Atlantic High pressure system and westerly winds to the south leading to a weakening (strengthening) of upwelling favourable south-easterly wind along the coast south of 33°S. Those changes in south-easterly wind weaken (strengthen) the upwelling and induce a warm (cold) SST anomaly along the west coast of Southern Africa. However, the direct link between ENSO, the wind and the SST is not so straightforward. For example, we could not find a wind proxy to match the first PC which is well correlated with ENSO. Moreover, while good correlations are found in summer between *in situ* wind at Cape Point and ENSO, no significant correlations were found at Cape Town airport. The local wind at the airport and ENSO were well correlated with the two first PC, a least during summer, and since the PCs are orthogonal modes, they should not be correlated. We therefore suggest that the first PC is partly led by large scale changes in the wind field impacted by ENSO (which might be partly captured at Cape Point) while the second PC is influenced by local variability of the wind (which is well captured at the airport).

The change in the net heat loss at the ocean surface due to sensible and latent heat fluxes could also impact the large scale

response of the region to ENSO (Colberg et al., 2004). Within False Bay and the region, investigation should be carried out to better understand the link between the SST inter-annual variability, ENSO, the synoptic atmospheric circulation, the local net heat fluxes and winds. The origin of the non-linearity between ENSO and the SST of the region is also a key issue to focus on.

This study shows that a certain degree of predictability is now offered at the scale of a bay, especially given the fact that the strongest correlation occurs during the mature phases of ENSO. Additionally, the local SST manually measured at Gordons Bay and the wind measurement at the airport and Cape Point has proven to be valuable and should be continued.

Acknowledgements — Funding for this work was provided by NRF, WRC, Nansen Tutu Center for environmental research, ACCESS and University of Cape Town. This manuscript is a contribution to the SEACHANGE NRF program, the MARE-BASICS program and SATREPS. The authors thank Christo Whittle for its help on the MODIS data processing and Angela Mead for her helpful review.

References

- Agenbag, J., 1996. Pacific ENSO events reflected in meteorological and oceanographic perturbations in the southern Benguela system. *South African Journal of Science* 92, 243–247.
- Andrew, W.R.H., Hutchings, L., 1980. Upwelling in the Southern Benguela Current. *Progress in Oceanography* 9 (1), 1–81.
- Atkins, G., 1970a. False Bay Investigations 1963–1970. Final report from the Marine Effluent Research Unit, Institute of Oceanography, University of Cape Town.
- Atkins, G., 1970b. Thermal structure and salinity of False Bay. *Transactions of the Royal Society of South Africa* 39, 117–128.
- Botes, W., 1988. Shallow water current meters comparative study: False Bay. CSIR Report T/SEA 880, 14.
- Brown, A., Davies, B., Day, J., Gardner, A., 1991. Chemical pollution loading of False Bay. *Transactions of the Royal Society of South Africa* 47 (4–5), 703–716.
- Colberg, F., Reason, C., Rodgers, K., 2004. South Atlantic response to El Niño Southern Oscillation induced climate variability in an ocean general circulation model. *Journal of Geophysical Research* 109, C12015.
- Cram, D., 1970. A suggested origin for the cold surface water in central False Bay. *Transactions of the Royal Society of South Africa* 39, 129–137.
- Demarcq, H., Barlow, R., Shillington, F., 2003. Climatology and variability of sea surface temperature and surface chlorophyll in the Benguela and Agulhas ecosystems as observed by satellite imagery. *African Journal of Marine Science* 25, 363–372.
- Dufois, F., Penven, P., Whittle, C., Veitch, J., 2012. On the warm nearshore bias in Pathfinder monthly SST products over Eastern Boundary Upwelling Systems. *Ocean Modelling* 47, 113–118.
- Fauchereau, N., Pohl, B., Reason, C., Rouault, M., Richard, Y., 2009. Recurrent daily OLR patterns in the Southern Africa/ Southwest Indian Ocean region, implications for South African rainfall and teleconnections. *Climate Dynamics* 32 (4), 575–591.
- Gründlingh, M., Largier, J., 1991. Physical oceanography of False Bay: a review. *Transactions of the Royal Society of South Africa* 47 (4–5), 387–400.
- Gründlingh, M., Potgieter, E., 1993. Unique thermal record in False Bay. *South African Journal of Science* 89, 510–512.
- Gründlingh, M., Hunter, I., Potgieter, E., 1989. Bottom currents at the entrance to False Bay, South Africa. *Continental Shelf Research* 9, 1029–1048.
- Horstman, D., McGibbon, S., Pitcher, G., Calder, D., Hutchings, L., Williams, P., 1991. Red tides in False Bay, 1959–1989, with particular reference to recent blooms of *Gymnodinium* sp. *Transactions of the Royal Society of South Africa* 47, 611–628.
- Jury, M.R., 1984. Wind shear and differential upwelling along the SW tip of Africa. PhD thesis, University of Cape Town.
- Jury, M.R., 1985. Mesoscale variations in summer winds over the Cape Columbine–St Helena Bay region, South Africa. *South African Journal of Marine Science* 3 (1), 77–88.
- Jury, M.R., 1986. The sudden decay of upwelling off the Cape Peninsula, South Africa: a case study. *South African Journal of Marine Science* 4 (1), 111–118.
- Kilpatrick, K., Podesta, G., Evans, R., 2001. Overview of the NOAA/NASA advanced very high resolution radiometer Pathfinder algorithm for sea surface temperature and associated matchup database. *Journal of Geophysical Research* 106, 9179–9197.
- Largier, J., Chapman, P., Peterson, W., Swart, V., 1992. The western Agulhas Bank: circulation, stratification and ecology. *South African Journal of Marine Science* 12 (1), 319–339.
- Lee, T., McPhaden, M., 2010. Increasing intensity of El Niño in the central-equatorial Pacific. *Geophysical Research Letters* 37, L14603.
- Legendre, P., Legendre, L., 1998. Numerical ecology. Elsevier Science Ltd.

- Lutjeharms, J., 1991. Surface front of False Bay and vicinity. *Transactions of the Royal Society of South Africa* 47 (4-5), 433–445.
- Lutjeharms, J., Cooper, J., 1996. Interbasin leakage through Agulhas Current filaments. *Deep Sea Research* 1 43, 213–238.
- Nelson, G., Cooper, R., Cruickshank, S., 1991. Time-series from a current-meter array near Cape Point. *Transactions of the Royal Society of South Africa* 47 (4-5), 471–482.
- Phillippon, N., Rouault, M., Richard, Y., Favre, A., 2011. The influence of ENSO on winter rainfall in South Africa. *International Journal of Climatology* <http://dx.doi.org/10.1002/joc.3403>.
- Pitcher, G., Stewart, B., Ntuli, J., 2008. Contrasting bays and red tides in the southern Benguela upwelling region. *Journal of the Oceanography Society* 21 (3), 82–91.
- Rouault, M., Richard, Y., 2003. Spatial extension and intensity of droughts since 1922 in South Africa. *Water SA* 29, 489–500.
- Rouault, M., Richard, Y., 2005. Intensity and spatial extent of droughts in Southern Africa. *Geophysical Research Letters* 32, L15702, <http://dx.doi.org/10.1029/2005GL022436>.
- Rouault, M., Pohl, B., Penven, P., 2010. Coastal Oceanic climate change and variability from 1982 to 2009 around South Africa. *African Journal of Marine Science* 32 (2), 237–246.
- Saha, S., Moorthi, S., Pan, H.L., Wu, X., Wang, J., Ncsaadiga, S., Tripp, P., Kistler, R., Woolen, J., Behringer, D., Liu, H., Stokes, D., Grumbine, R., Gayno, G., Wang, J., Hou, Y.T., Chuang, H., Juang, H.M.J., Sela, J., Irdell, M., Treadon, R., Klesits, S., Felst, P.V., Keyser, D., Derber, J., Ek, M., Meng, J., Wei, H., Yang, R., Lord, S., van den Dool, H., Kumar, A., Wang, W., Long, C., Chelliah, M., Xue, Y., Huang, B., Schemm, J., Ebisuzaki, W., Lin, R., Xie, P.P., Chen, M., Zhou, S., Higgins, W., Zou, C.Z., Liu, Q., Chen, Y., Han, Y., Cucurull, L., Reynolds, R.W., Rutledge, G., Goldberg, M., 2010. The NCEP climate forecast system reanalysis. *Bulletin of the American Meteorological Society* 91, 1015–1057.
- Shannon, L., Chapman, P., 1983. Suggested mechanism for the chronic pollution by oil of beaches east of Cape Agulhas, South Africa. *South African Journal of Marine Science* 1, 231–244.
- Shannon, L., Walters, N., Moldan, A., 1983. Some features in two Cape bays as deduced from satellite ocean-colour imagery. *South African Journal of Marine Science* 1, 111–122.
- Shannon, L., Walters, N., Mostert, S., 1985. Satellite observations of surface temperature and near-surface chlorophyll in the southern Benguela region. In: Shannon (Ed.), *South African Ocean Colour Experiment*, Sea Fisheries Research Institute, Galvin and Sales, Cape Town, pp. 183–210.
- Skibbe, E., 1991. Impact assessment of the sewage effluent at Zeekoevlei. *Transactions of the Royal Society of South Africa* 47 (4-5), 716–730.
- Taljaard, S., Ballegooyen, R.V., Morant, P., 2000. False Bay Water Quality Review, Volume 2: Specialist Assessments and Inventories of Available Literature and Data, Report to the False Bay Water Quality Advisory Committee. CSIR Report ENV-S-C 2000-086/2 2.